B-cell immunity and vaccine induced antibody protection reveal the inefficacy of current vaccination schedule in infants with perinatal HIV-infection in Mozambique, Africa

Nicola Cotugno,[a,b,h] Suresh Pallikkuth,[c,h] Marco Sanna,[a,b] Vinh Dinh,[c] Lesley de Armas,[c] Stefano Rinaldi,[c] Sheldon Davis,[c] Giulia Linardos,[d] Giuseppe Rubens Pascucci,[a,b] Rajendra Pahwa,[c] Nadia Sitoe,[e] Paula Vaz,[f] Paolo Rossi,[b,g] Maria Grazia Lain,[e] Paolo Palma,[a,b,h,**] and Savita Pahwa[c,h,*]

[a]Clinical Immunology and Vaccinology Unit, Bambino Gesù Children's Hospital, IRCCS, Rome 00165, Italy
[b]Chair of Pediatrics, Department of Systems Medicine, University of Rome "Tor Vergata", Rome 00133, Italy
[c]Department of Microbiology and Immunology, Miami Center for AIDS Research, Miller School of Medicine, University of Miami, Miami, United States
[d]Microbiology and Diagnostic Immunology Unit, Bambino Gesù Children's Hospital, IRCCS, Piazza Sant'Onofrio, 4, Rome 00165, Italy
[e]Fundação Ariel Glaser Contra o SIDA Pediatrico, Maputo, Mozambique
[f]Instituto Nacional de Saúde, Marracuene, Maputo Province, Mozambique
[g]Chair of Pediatrics, Bambino Gesù Children's Hospital, IRCCS, Rome 00165, Italy

eBioMedicine
2023;93: 104666
Published Online 3 July 2023
https://doi.org/10.1016/j.ebiom.2023.104666

Summary

Background Despite antiretroviral treatment (ART), immune dysfunction persists in children with perinatal HIV infection (HEI). Here we investigated the impact of HIV status on maternal antibody (Ab) passage, long-term vaccine induced immunity and B-cell maturation.

Methods 46 HIV Exposed Uninfected (HEU), 43 HEI, and 15 HIV unexposed uninfected (HUU) infants were vaccinated with 3 doses of DTaP-HepB-Hib-PCV10-OP at 2, 3, and 4 months at Matola Provincial Hospital, Maputo, Mozambique. Tetanus toxoid specific (TT) IgG, HIV Ab and B-cell phenotype characteristics were evaluated at entry, pre-ART, 5, 10, and 18 months in this longitudinal cohort study.

Findings Baseline (maternal) plasma TT Ab levels were significantly lower in HEI compared to both HEU and HUU and a faster decay of TT Ab was observed in HEI compared to HEU with significantly lower TT Ab levels at 10 and 18 months of age. TT unprotected (UP) (≤0.1 IU/mL) HEI showed higher HIV-RNA at entry and higher longitudinal HIV viremia (Area Under the Curve) compared to TT protected (P) HEI. A distinct HIV-Ab profile was found at entry in HEI compared to HEU. B-cell phenotype showed a B-cell perturbation in HEI vs HEU infants at entry (mean age 40.8 days) with lower transitional CD10+CD19+ B-cells and IgD+CD27− naive B-cells and an overall higher frequency of IgD−CD27− double negative B-cell subsets in HEI.

Interpretation B-cell perturbation, presenting with higher double negative IgD−CD27− B-cells was observed in neonatal age and may play a major role in the B-cell exhaustion in HEI. The ability to maintain TT protective Ab titers over time is impaired in HEI with uncontrolled viral replication and the current vaccination schedule is insufficient to provide long-term protection against tetanus.

Funding This work was supported by: NIH grant to SP (5R01AI127347-05); Children's Hospital Bambino Gesú (Ricerca corrente 2019) to NC, and Associazione Volontari Bambino Gesù to PP.

Keywords: Pediatric HIV; Vaccine induced immunity; Tetanus responses; Memory B-Cells; B-cell aging; Double negative B-cells

*Corresponding author. Department of Microbiology and Immunology, University of Miami, Miami, United States.
**Corresponding author. Clinical Immunology and Vaccinology Unit, Children Hospital Bambino Gesù, IRCCS, University of Rome "Tor Vergata", Rome, Italy.
E-mail addresses: spahwa@med.miami.edu (S. Pahwa), paolo.palma@opbg.net (P. Palma).
[h]Contributed equally to the manuscript.

Research in context

Evidence before this study

Despite long-term viral suppression due to effective ART, B-cell perturbation experienced by persons living with HIV may persist and contribute to a lower ability to induce and maintain memory responses for vaccine preventable diseases. Previous analysis on cross sectional data revealed a lower vaccine induced seroprotection upon routine immunization in children living with HIV. However, timing of vaccine induced immunity persistence and of B cell immune exhaustion remain unknown in children with perinatal HIV infection.

Added value of this study

This study provides a longitudinal evaluation of tetanus response upon routine immunization in a cohort of children living with HIV and uninfected children born to mothers living with HIV in a cohort in southern Mozambique (the TARA cohort). Data collected at 40 days of life show that 50% of children living with HIV do not have maternally derived Tetanus Ab compared to 25% of exposed uninfected and 6% of unexposed uninfected children. A similar perturbation was further confirmed at 9 and at 18 months of age, especially in children with higher plasma HIV-RNA. A distinct maternal HIV antibody (Ab) passage was further shown in children living with HIV where a distinct HIV Ab footprint was found compared to exposed uninfected children.

An in-depth immunological B cell characterization in infants with HIV infection showed a paradoxical perturbation, characterized by a higher frequency of a B-cell subset so far known to be increased in aging or inflammatory conditions or in other infectious diseases such as cytomegalovirus and malaria. Such a B cell subset characterized by the absence of maturational molecules CD27 and IgD, and previously shown after years of HIV exposure, was present in the children at a very early phase (40 days of life). A machine learning approach, albeit limited by the small sample size, revealed how memory B cell subsets at entry could predict the ability of children living with HIV to maintain a protective vaccine induced titer at 10 months of age.

Implications of all the available evidence

These data provide evidence for the inability of children living with HIV to maintain protective antibody titers following the current vaccination schedule for tetanus in Mozambique. The present longitudinal study comprehensively determined the evolution of B-cells over the first 2 years of life and revealed a hallmark of immune activation and exhaustion in infants living with HIV since the age of 40 days. These data further confirm the impact of HIV on vaccine induced memory and suggests that B-cell immune profiling may be used in the future as a predictive factor able to personalize the vaccination schedule of HIV-infected children.

Introduction

With implementation of ART for prevention of human immunodeficiency virus (HIV) transmission from mother to child, the majority of children born to women with HIV do not acquire perinatal HIV-infection. Of those children who are infected, most acquire the virus from their mothers at the time of delivery or shortly thereafter by breast-feeding. Despite long-term viral suppression due to effective ART and humoral impairment experienced in persons with HIV, B-cell perturbation may persist and contribute to a lower ability to induce Ab and maintain immunologic memory responses against vaccine preventable diseases.[1–3] This persistent perturbation is commonly attributed to a "inflammaging" process which was shown by a substantial expansion of pro inflammatory B-cell subsets[4–6] in addition to a persistently lower memory B-cells (IgD–CD27+) and resting memory B-cells (IgD–CD27+CD21+).[2,7] Besides B-cell associated perturbation found in children with HIV, alterations in transplacental passage of maternal IgG, previously shown to be influenced by maternal humoral perturbation,[8] may result in lower protection from vaccine preventable diseases in the vulnerable neonates. We here focused our analysis on tetanus Ab response, which still represents a challenging vaccine preventable disease to eradicate. In 2015, 79% of deaths due to tetanus (44'612 of 56'743) regardless of HIV status were estimated to occur in south Asia and sub-Saharan Africa.[9]

Here we investigated the longitudinal development of B-cells and B-cell perturbation in children with perinatal HIV infection from 1 month up to 18 months of age in a cohort enrolled in Maputo, Mozambique, Africa named TARA (Toward AIDS Remission Approaches). We further investigated the response and maintenance of tetanus vaccine induced humoral response and baseline predictors of good vaccine-induced immunity in children living with HIV.

Methods

Study participants

HIV exposed uninfected infants (HEU), infants with perinatal HIV infection (HEI) and HIV Unexposed infants (HUU) were recruited at 1–2 months of age and followed at Matola Provincial Hospital in Maputo, Mozambique and followed between February 2017 and October 2020. HEU continued the post-natal prophylaxis with Nevirapine (NVP), while HEI started ART at the time of HIV diagnosis with Zidovudine (AZT) or Abacavir (ABC) plus Lamivudine (3TC) and Lopinavir/Ritonavir (LPV/r). HIV diagnosis was determined by 2 positive PCR tests using Alere™ q HIV-1/2 molecular

diagnostic platform within the second month of age. Infants with two positive virologic tests were classified as HEI and infants with negative virologic tests were classified as HEU, while HUU were infants born to mothers with negative HIV test results.

All infants received vaccinations as designated by local recommendations including BCG, DTaP-HepB-Hib-PCV10-OP at 2, 3 and 4 months and measles-rubella vaccine at 9 and 18 months of age. Whole blood was collected before starting ART and at 1, 2, 5, 9, 10, 17 and 18 months after ART initiation Lost to follow up and numbers of deceased participants over time have been previously reported.[10,11] All study partcipants reported had a full compliance to TT vaccination. Study design has now been showed in Supplementary Fig. S1.

HIV viral load determination and CD4 counts

HIV-1 Plasma viral load was quantified using COBAS® AmpliPrep/COBAS® TaqMan® HIV-1 Test, version 2.0 (Roche Diagnostics, Germany) with a limit detection of 20 copies/ml, and Ampliprep CAP/CTM analyzer.

Absolute Lymphocyte/CD4 counts were quantified using BD Multitest™ anti-CD3FITC/anti-CD8PE/anti-CD45PerCP/anti-CD4APC and TruCount tubes (Becton Dickinson, USA) and analyzed in FACSCalibur flow cytometry (Becton Dickinson, USA).

Ethics statement

The study was approved by the Mozambique National Bioethical Committee (IRB00002657, reference 102/CNBS/2016) and the Ministry of Health (MOH) of Mozambique (MISAU) and by the Institutional Review Board of University of Miami (IRB00010711). All Infants' caregivers consented the participation in the study through written signed informed consent.

Sample collection and storage

Venous blood was collected and processed within 2 h and plasma was stored at –80 °C. Peripheral blood mononuclear cells (PBMCs) were isolated by Ficoll and cryopreserved in liquid nitrogen.

Humoral response to tetanus and HIV

HIV-1 Ab were analyzed by Western blot analysis (WB) (Medical Systems, Italy) and WB score was calculated as previously shown.[12] WB blots are available in Supplemental Western Blot. Tetanus IgG titers were performed by EUROIMMUN ELISA (EUROIMMUN-Italia, Padova, Italy) (cat. no. EI 2060-9601G) and Measles IgG titers were evaluated by EUROIMMUN ELISA (EUROIMMUN-Italia, Padova, Italy) (cat. no. EI 2610-9601G) and evaluated according to serologic titers of protection.[13]

B-cell phenotype analysis

Cryopreserved PBMC were thawed and rested overnight in RPMI-1640 with 10% FBS, 1% Pen-Strep, and 1% Glutamine, blocked with Human TruStain FcX (Biolegend) and stained with previously titrated monoclonal antibodies (listed in Supplementary Table S1 and gating strategy in Supplementary Fig. S2). Stained PBMC were fixed and acquired on a Cytek Aurora Flow Cytometer and analyzed by FlowJo software (version 10.8.1).

Statistical analysis

Unless otherwise noted, statistical analysis was performed using R (version 4.2.2) or Python (version 3.8.10). The choice of the most appropriate statistical test was performed according to data distribution. Normality assumption was tested by the Shapiro Wilk test and homogeneity of variance was validated by Levene's test. For sample size calculation, power analysis was performed using effect size informed by *Cohen's d* according to tetanus Ab response after vaccination (5 months) in HIV exposed and HIV infected children (effect size = 0.68). Accordingly, a sample size of 35 per group estimates to achieve 80% power using a two-tailed t-test at 0.05 alpha level. Given that our Mozambique cohort consisted of more than 40 HEI and more than 40 HEU we estimated an ample power to test hypotheses included in the project. Differences between groups were tested using the Welch T test (two-tailed) if both distributions were normal, or conversely, with the non-parametric Mann–Whitney U test. Fisher's exact test (two-tailed) was applied to test differences in categorical data. Missing values were filtered out of the analysis. P-values of <0.05 were considered significant and the Bonferroni correction was applied to control the family-wise error rate (FWER) when multiple comparisons were performed. A full report of statistical results, including n values for groups and time points is available in a Mendeley repository file (https://doi.org/10.17632/b3d2p9fzg3.1). An Exploratory Data Analysis (EDA) was performed and Principal Component Analysis (PCA) was used as a modeling approach to reduce the number of variables in analysis and to summarize the most important information to identify the key drivers of variation in the data.

Prediction score by XGBoost classification

A machine learning approach was applied to identify whether 10 months TT vaccine-induced immunity in HEI could be predicted using baseline data (B-cell phenotype, clinical data, and HIV related data). We compared the performance of 27 different classification algorithms via LazyPredict (version 0.2.12). Best performing models were selected based on a tradeoff between Accuracy, ROC AUC and F1 score metrics when tested on a 60/40 (train/test) split. XGBoost (XGB) classification algorithm, which is a scalable end-to-end tree boosting system that can and capture non-linear relationships between the features and the target variable, was chosen for the construction of the final model. A matrix of paired HEI baseline data and the TT vaccine

protection outcome at 10 months were used as input in xgboost (version 1.7.4).[14] Incomplete data were filtered out and due to the remaining limited sample size (n = 22), we opted for a nested Leave One Out Cross Validation (LOO-CV) approach[15] to maximize performance in training and testing the final model. A nested LOO-CV approach is an effective way to address the issue of small sample size by maximizing the amount of data used for model training while still being able to test the model's performance on unseen data. This method involves repeatedly splitting and testing the data using a leave-one-out strategy. This process is repeated until every observation has been used as a test set. The first inner cross validation layer is used to optimize the model's hyperparameters (learning_rate, max_depth, min_child_weight, n_estimators, reg_alpha, reg_lambda, and subsample) using hyperopt software (version 0.2.5),[16] and the second inner cross validation layer is used to select the best set of features to train the model using sklearn (version 1.0.2) recursive feature elimination algorithm RFECV.[17] SHAP (SHapley Additive exPlanations)[18] values were used to explain the contribution of each selected feature in the model towards the prediction. SHAP attributes a fair value to each feature by considering all possible combinations of features, the sum of all feature values is equal to the prediction output. The same approach at later timepoints (18 and 19 months of age) could not be tested due to the small sample size.

Results

Patients' characteristics

The studies were conducted in 43 infants diagnosed with HIV (HEI), and 46 HIV exposed uninfected (HEU) and an additional group of 15 HIV unexposed uninfected (HUU). Clinical, virological and immunological parameters, as well as number of participants enrolled per visit are reported in Table 1. Mean age at entry was 40 days and no differences in terms of age and gender were reported between the study groups (Table 1). Weight was significantly lower in HEI (μ = 4.03, 95% CI [3.8, 4.25]) compared to HEU (μ = 4.44, 95% CI [4.18, 4.69]; p = 0.017) and this difference persisted up to 9 months of age.

Ab maternal passage and vaccine induced Ab response in HEU and HEI

Baseline Ab levels at study entry, presumed to be maternally transferred as well as vaccine induced Ab responses were investigated in longitudinal samples of HEU and HEI. Tetanus responses at entry were also compared with HUU samples. We found lower maternally derived Tetanus (TT) antibodies in HEI (n = 34, μ = 0.33, 95% CI [0.18, 0.48]) compared to HEU (n = 36, μ = 0.66, 95% CI [0.41, 0.91]) (p = 0.002) (Fig. 1A). Indeed 17 out of 34 HEI (50%) analyzed for TT Abs at entry showed no protective titer (≤0.1 mIU/mL) compared to 9 out of 36 (25%) in HEU and 1 out of 15 (6.5%) in HUU (see table in Fig. 1A). HUU infants presented significantly higher TT Ab levels (μ = 1.94, 95% CI [1.15, 2.73]) compared to both HEI and HEU (p < 0.001 for both). For both HEI and HEU a good response at 5 months of age upon TT vaccination was found with a higher titer in HEI (μ = 2.06, 95% CI [1.67, 2.45]) compared to HEU (μ = 1.40, 95% CI [1.14, 1.65]) (p = 0.006). TT Ab titer was further investigated at 9, 10, 18 and 19 months of age and overall data showed that HEI present a more pronounced waning compared to HEU, with significantly lower TT Ab titers at 10 months (HEI: μ = 0.68, 95% CI [0.48, 0.87]; HEU: μ = 0.99, 95% CI [0.78, 1.94]) and at 18 months of age (HEI: μ = 0.5, 95% CI [0.29, 0.71]; HEU: μ = 0.76, 95% CI [0.51, 1.00]) (Mann Whitney test p = 0.019 and 0.039 respectively) further confirmed by linear mixed effect model (Supplementary Fig. S3A). These data regarding the lower ability to maintain vaccine induced Ab were confirmed by lower measles Ab at the time of the booster dose (18 months of age) in HEI compared to HEU (Supplementary Fig. S3B).

HIV specific humoral response in HEI and HEU

To investigate the HIV Ab maternal passage, Western blot analysis of 10 distinct HIV Ag was investigated at entry and at 10 months of age in HEU and at all timepoints in HEI (entry, 5, 9, 10, 18, 19 months). The Western blot score (WB score[10]), was similar at entry between the groups (Fig. 1B) and waned at 10 months in both groups with a significantly lower WB score in HEU (μ = 0.68, 95% CI [0.44, 0.92]) compared to HEI (μ = 2.2, 95% CI [1.59, 2.81]) (p < 0.001). From a qualitative perspective, Western blot analysis showed a distinct repertoire of HIV Antibodies in HEI compared to HEU. Indeed, at entry gp160 Ab were significantly higher in HEI, whereas p55 and p17 Abs were higher in HEU compared to HEI (Fig. 1C). No differences were found for HIV Ab specific to p66, p24, gp120, p51, p39 and p31 between HEI and HEU at entry (Fig. 1C). HIV Ab analysis at 10 months of age showed an overall reduction in HIV Ab with the persistence of higher levels in p24, gp120, gp41 and gp160 in HEI compared to HEU (Fig. 1D), suggesting these values to be autologous Ab rather than deriving from maternal passage. In order to investigate whether the HIV Ab could differ in infants with distinct maternal passage of TT Ab, HIV WB score was investigated in TT protected at entry (≥0.5 IU/mL) (TT P) compared to TT unprotected (<0.5 IU/mL) (TT UP) (Fig. 1E). A higher mean Western blot score was found in TT UP at 9 months of age compared to TT P (p = 0.03) (Supplementary Fig. S3C). Same result, albeit not significant presumably due to the smaller sample size, was found in TT UP (μ = 2.82, 95% CI [1.83, 3.8]) compared to TT P (μ = 1.84, 95% CI [1.09, 2.59]) at 10 months (Fig. 1E–G). Relation between

	Entry (n = 89)			5 months (n = 78)			9 months (n = 75)			18 months (n = 69)		
	HEU (n = 46)	HEI (n = 43)	P-value	HEU (n = 40)	HEI (n = 38)	P-value	HEU (n = 39)	HEI (n = 36)	P-value	HEU (n = 34)	HEI (n = 35)	P-value
Sex												
Male (Female)	22 (24)	17 (26)	0.52	19 (21)	14 (24)	0.37	19 (20)	14 (22)	0.47	17 (17)	14 (21)	0.47
Age (days)												
Mean (sd)	39.97 (12.84)	40.79 (13.68)	0.7	152.5 (7.32)	153.47 (5.27)	0.6ì	276 (4.49)	273.05 (4.26)	0.005	549.91 (5.17)	549.0 (5.01)	0.09
Weight (kg)												
Mean (sd)	4.44 (0.84)	4.03 (0.73)	0.017	7.25 (1.11)	6.47 (1.17)	0.003	8.56 (0.96)	7.94 (1.08)	0.01	10.08 (1.11)	9.51 (1.23)	0.051
Height (cm)												
Mean (sd)	53.34 (3.28)	52.39 (2.95)	0.16	63.25 (2.61)	61.58 (2.76)	0.008	69.67 (2.65)	67.47 (2.32)	<0.001	76.37 (2.88)	76.77 (3.37)	0.6
Age at ART initiation (days)												
Mean (sd)	*n.a.*	40.28 (14.02)	/	*n.a.*	40.71 (14.26)	/	*n.a.*	38.72 (11.51)	/	*n.a.*	38.34 (11.46)	/
Days to viral suppression	*n.a.*	[19/43]	/	*n.a.*	[18/38]	/	*n.a.*	[19/36]	/	*n.a.*	[19/35]	/
(≤20 cp/mL) $\left[\frac{N_{Suppr}}{N_{tot}}\right]$, mean (sd)		351.79 (170.93)			354.27 (175.28)			351.79 (170.93)			351.79 (170.93)	
Days to viral suppression	*n.a.*	[25/43]	/	*n.a.*	[24/38]	/	*n.a.*	[25/36]	/	*n.a.*	[25/35]	/
(≤400 cp/mL) $\left[\frac{N_{Suppr}}{N_{tot}}\right]$, mean (sd)		291.52 (299.23)			290.87 (305.39)			291.52 (299.23)			291.52 (299.23)	
AUC HIV-RNA (cp/mL)												
Mean area (sd)	*n.a.*	n.a.	/	*n.a.*	$6.97{\cdot}10^{6}$ ($8.38{\cdot}10^{6}$)	/	*n.a.*	$8.84{\cdot}10^{6}$ ($1.28{\cdot}10^{7}$)	/	*n.a.*	$1.29{\cdot}10^{7}$ ($2.05{\cdot}10^{7}$)	/
HIV-RNA (cp/mL)												
Mean (sd)	*n.a.*	$3.01{\cdot}10^{6}$ ($3.80{\cdot}10^{6}$)	/	*n.a.*	$1.07{\cdot}10^{6}$ ($2.49{\cdot}10^{6}$)	/	*n.a.*	$7.55{\cdot}10^{56}$ ($2.08{\cdot}10^{6}$)	/	*n.a.*	$1.65{\cdot}10^{56}$ ($5.45{\cdot}10^{56}$)	/
Peak viremia (cp/mL)												
Mean (sd)	*n.a.*	$4.60{\cdot}10^{6}$ ($4.12{\cdot}10^{6}$)	/	*n.a.*	$4.34{\cdot}10^{6}$ ($4.04{\cdot}10^{6}$)	/	*n.a.*	$4.07{\cdot}10^{6}$ ($3.97{\cdot}10^{6}$)	/	*n.a.*	$4.17{\cdot}10^{6}$ ($3.98{\cdot}10^{6}$)	/
CD4+ T cells %												
Mean (sd)	*n.a.*	33.59 (10.33)	/	*n.a.*	n.a.	/	*n.a.*	25.65 (9.97)	/	*n.a.*	32.66 (8.10)	/
WHO stage												
(I/II/III/IV)	*n.a.*	39/2/1/1	/	*n.a.*	32/4/1/1	/	*n.a.*	30/4/2/0	/	*n.a.*	25/6/4/0	/
ART therapy												
$N_{patients}$ (Drugs)	*n.a.*	32 (AZT+3TC+LPV/rit) 2 (ABC+3TC+LPV/rit) 0 (ABC+AZT+3TC) 1 (AZT+3TC+NVP) 8 (*n.a.*)	/	*n.a.*	27 (AZT+3TC+LPV/rit) 0 (ABC+3TC+LPV/rit) 0 (ABC+AZT+3TC) 1 (AZT+3TC+NVP) 10 (*n.a.*)	/	*n.a.*	18 (AZT+3TC+LPV/rit) 2 (ABC+3TC+LPV/rit) 0 (ABC+AZT+3TC) 0 (AZT+3TC+NVP) 16 (*n.a.*)	/	*n.a.*	5 (AZT+3TC+LPV/rit) 2 (ABC+3TC+LPV/rit) 1 (ABC+AZT+3TC) 0 (AZT+3TC+NVP) 27 (*n.a.*)	/

Table 1: **Patient's characteristics.**

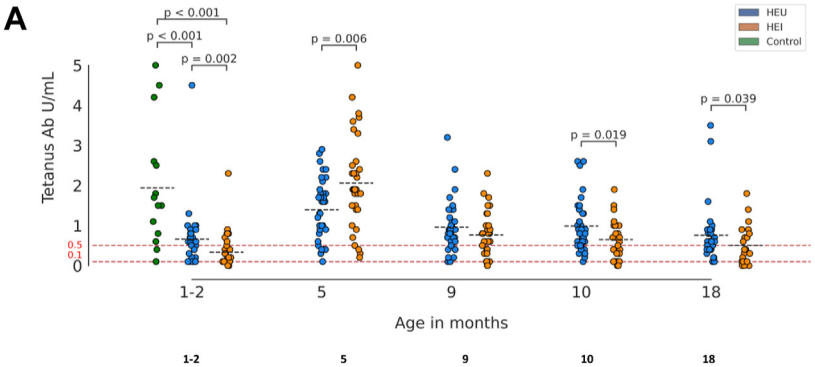

	1-2			5		9		10		18	
	CS	HEU	HEI	HEU	HEI	HEU	HEI	HEU	HEI	HEU	HEI
P	13 (87%)	23 (64%)	8 (24%)	30 (83%)	31 (91%)	31 (84%)	21 (68%)	31 (84%)	19 (63.3%)	22 (65%)	9 (41%)
B	1 (6.5%)	4 (11%)	9 (26%)	5 (14%)	3 (9%)	4 (11%)	4 (13%)	5 (13%)	4 (13.3%)	10 (29%)	5 (23%)
UP	1 (6.5%)	9 (25%)	17 (50%)	1 (3%)	0 (0%)	2 (5%)	6 (19%)	1 (3%)	7 (23.3%)	2 (6%)	8 (36%)

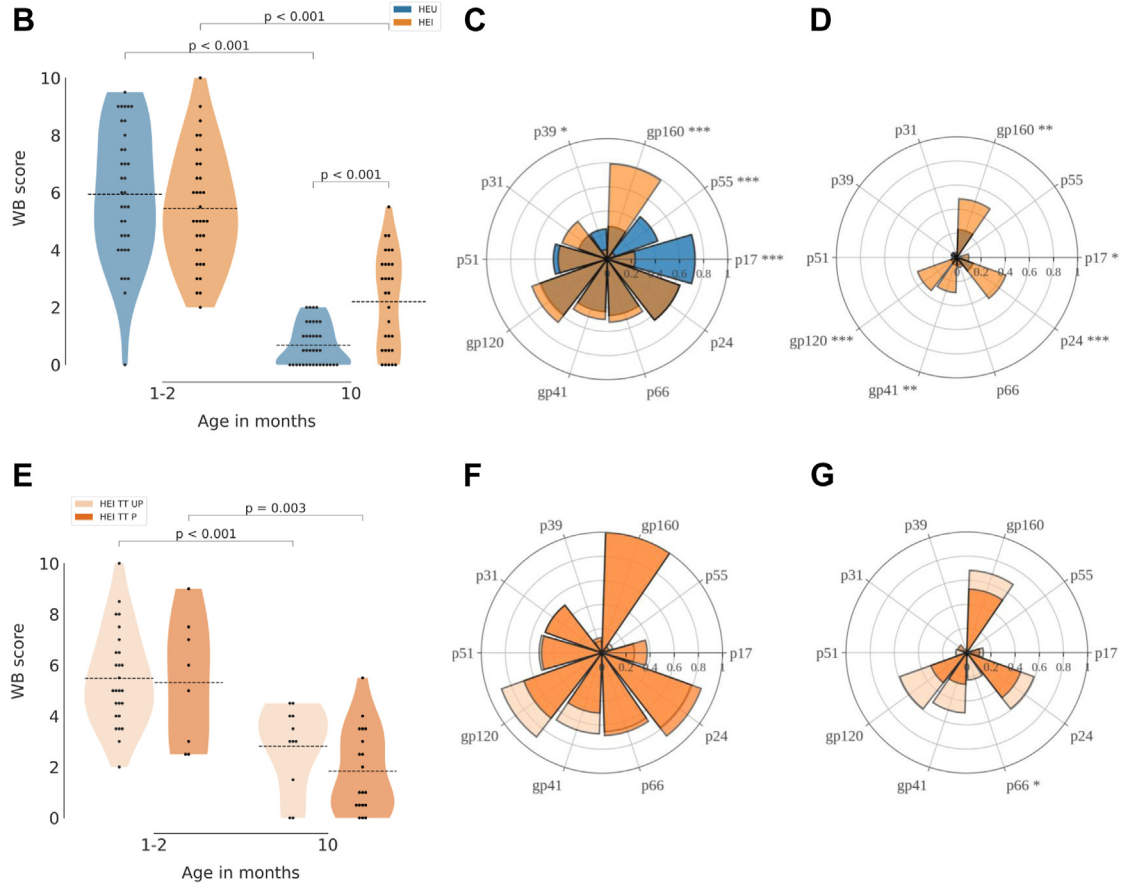

Fig. 1: **Tetanus and HIV Ab in newborns and over time.** Scatter plot in panel **A** shows longitudinal TT Ab response in HEU, HEI and HUU, with mean values as black dotted lines. Red dotted lines indicate threshold of protection (0.1 IU/mL) and the threshold for borderline of serologic protection (0.5 IU/mL). Table in panel **A** shows distribution among Protected individuals (≥0.5 IU/mL), Borderline (0.1 < x < 0.5 IU/mL), unprotected (≤0.1 IU/mL). Violin plots in panel **B** and **E** show the Western blot (WB) score calculated as described in the method section. Spider plots in panel **C, D, F, G** are calculated with a cumulative WB score, divided by the total number of patients for which the Ab measurement was performed. Differences between HEI and HEU in panels from A to G were calculated as described in Methods. Significant p-values across the distinct antigen of the spider plots are shown as asterisks (* = $p < 0.05$; ** = $p \leq 0.01$; *** = $p \leq 0.001$).

longitudinal HIV-RNA and HIV WB score is further singularly analyzed in all time points (Supplementary Fig. S4).

The impact of HIV replication on vaccine induced immunity

In order to investigate the impact of HIV replication on vaccine induced Ab response, a longitudinal analysis of HIV-RNA was performed between TT P and TT UP among the HEI group. Significantly higher HIV-RNA cp/mL in TT UP vs TT P were found at entry (TT UP: n = 8, $\mu = 3.58{\cdot}10^6$, 95% CI [$2.08{\cdot}10^6$, $5.08{\cdot}10^6$]; TT P: n = 26, $\mu = 1.46{\cdot}10^4$, 95% CI [0, $3.90{\cdot}10^6$]; p = 0.02) and at 9 months of age (TT UP: n = 10, $\mu = 2.38{\cdot}10^6$, 95% CI [$9.42{\cdot}10^4$, $4.67{\cdot}10^6$]; TT P: n = 21, $\mu = 7.60{\cdot}10^4$, 95% CI [0, $1.55{\cdot}10^5$]; p = 0.02) (Fig. 2A). HIV exposure, measured by the area under the curve of HIV-RNA, was significantly higher in TT UP compared to TT P in all time points (Fig. 2B). This result further suggests that HIV-RNA significantly impacts the vaccine induced Ab maintenance rather than Ab production after immunization. No differences were found in terms of CD4 T cell count and CD4 T cell percentages between TT UP and TT P (data not shown).

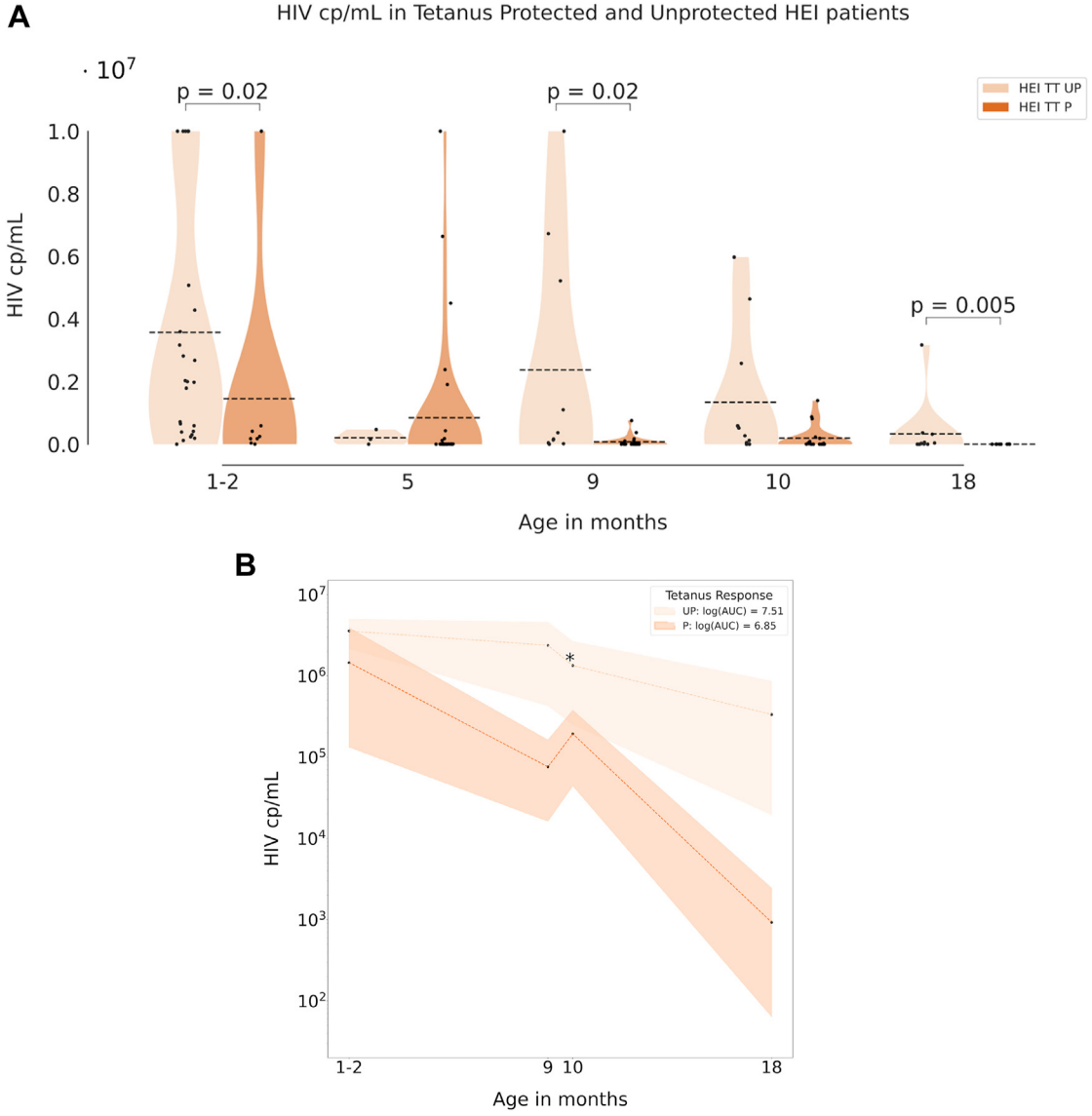

Fig. 2: **The impact of HIV on vaccine induced response.** Violin plots in panel **A** show the HIV RNA copies in HEI who were TT protected (P) or unprotected (UP); dotted lines indicate the mean. Panel **B** shows the area under the curve of the cumulative HIV RNA in UP and P patients. Differences at distinct time points between the groups are defined as described in Methods (* = $p \leq 0.05$; ** = $p \leq 0.01$; *** = $p \leq 0.001$).

Longitudinal evaluation of the B-cell compartment in HEI and HEU

Multiparameter flow cytometry analysis (FCM) was utilized to investigate B-cell phenotype at all time-points. The analysis of differentially expressed features (DEFs), which in our study represent B cell subsets, with statistically significant changes (adj. p-value < 0.05) in their frequency, showed major differences between HEI and HEU at entry compared to later time-points.

Out of the 330 B-cell phenotype features analyzed, 11 DEF (3%) were found at entry (1–2 months of age) compared to 2 and 3 DEF found respectively at 5 and 10 months of age (Fig. 3A). These data suggest that B-cell impairment occurs very early in life in HEI compared to HEU. Indeed, the B-cell subsets were skewed towards more mature B-cells in HEI compared to HEU with a significantly higher frequency of mature B-cells (CD19+CD10– live B-cells) (HEI: μ = 88.38, 95% CI [85.55, 91.22]; HEU: μ = 77.23, 95% CI [73.36, 81.10]; p = 0.003) and lower transitional (CD19+CD10+ live B-cells) (HEI: μ = 9.48, 95% CI [7.11, 11.85]; HEU: μ = 19.34, 95% CI [15.47, 23.20]; p = 0.005) and naïve B-cells (CD19+CD10–CD27–IgD+ live B-cells) (HEI: μ = 91.78, 95% CI [90.44, 93.11]; HEU: μ = 95.44, 95% CI [94.85, 96.03]; p = 0.006) (Fig. 3B). Both total double negative (CD19+IgD–CD27–; DN) B-cell (HEI: μ = 7.85, 95% CI [6.54, 9.16]; HEU: μ = 3.89, 95% CI [3.32, 4.45]) and CD21– DN (HEI: μ = 81.74, 95% CI [77.92, 85.55]; HEU: μ = 62.89, 95% CI [57.87, 67.89]) were significantly higher in HEI compared to HEU (p < 0.001 for both subsets) (Fig. 3B). In contrast, the unswitched memory B-cell subset (CD19+CD27+IgD+CD21+) at entry was significantly higher in HEU (μ = 0.28, 95% CI [0.22, 0.35]) compared to HEI (μ = 0.11, 95% CI [0.08, 0.15]) (p = 0.007) (Fig. 3C).

The B-cell phenotype at entry was further evaluated by principal component analysis (PCA). As shown in Fig. 3D, PC5 was able to discriminate between HEU and HEI and performed better compared to other components analyzed (data not shown). The top loading features driving the PC5 are shown in Fig. 3E (bottom panel). Six out of the ten top loading features fall within the DN B-cell subsets between HEI and HEU at a very early stage of life.

B-cell maturation in the first 18 months of life differs between HEI and HEU

To investigate the impact of age on the B-cell evolution in the entire cohort, and in both HEU and HEI, PCA was performed on B-cell phenotype data (Supplementary Fig. 5A–C, respectively). PC1, was able to discriminate samples by age when both HEI and HEU data were included into the analysis. Top loading contributors were within the DN B-cells (Supplementary Fig. S5A). Surface markers indicative of B-cell maturation and activation after Ag encounter, such as CD21, IgM and IgG out of total DN B-cells, were contributing to PC1 and in turn to B-cell maturation in both groups. Specifically, IgG, CD21, out of total DN found in later time points and IgM+ and CD21– and CD38+ in younger children.

To further investigate whether the aging process of the B-cell compartment was differentially driven according to the HIV status, PCA deriving from B-cell phenotype data was investigated separately at all time points for HEU (Supplementary Fig. S5B) and HEI (Supplementary Fig. S5C). For both groups PC1 was able to discriminate age at sampling (Supplementary Fig. S5 D and E). For HEI, bubble plot in Supplementary Fig. S5C further shows the HIV RNA at sampling. As expected, due to the natural history of the HIV perinatal infection and due to the impact of ART, larger bubbles were found in early time points. The analysis of top contributors revealed a different set of B-cell subsets driving aging in HEI and HEU. Whereas in HEU 5 out of the 10 top contributors were within the switched memory, B-cell memory and only 4 contributors were within the DN B-cell subsets. In HEI, 9 (90%) out of 10 top contributors to aging were within the DN B-cell subsets further confirming the importance of this B-cell subset in the perturbed aging of the B-cells of children living with HIV.

Baseline predictors of TT response in HEI revealed by machine learning

To identify whether the TT vaccine-induced protection observed at 10 months in HEI could be predicted based on baseline data (B-cell phenotype, clinical data, and HIV related data), we compared the performance of different classification algorithms with default parameters. Quadratic Discriminant Analysis (QDA), a supervised learning algorithm that models the distribution of each class with a quadratic surface, and XGBoost (XGB) classification algorithm, which is a scalable end-to-end tree boosting system, achieved the best performances (Fig. 4, panel 2). Considering the small sample size (n = 22), we selected XGBoost for the construction of the final predictive model. A matrix of HEI baseline data and the TT vaccine protection outcome at 10 months were used as input for XGBoost classification in xgboost (version 1.7.4). The final model was trained using the best parameters and features selected during the optimization process ('learning_rate': 0.04, 'max_depth': 9.0, 'min_child_weight': 3.0, 'n_estimators': 226.0, 'reg_alpha': 0.93, 'reg_lambda': 0.73, 'subsample': 0.7), resulting in an improvement of the unoptimized model with an average accuracy score of 81.8 (±38.6) % on the test (Fig. 4, panel 2). The model showed an accuracy (measured as F1 score, which is the harmonic mean of precision and recall) of 0.897 (90%) in predicting TT protection at 10 months, with three patients out of 22 HEI being mispredicted, one false negative and two false positive (Fig. 4, panel 3). The top contributors for the score were subsets within the memory compartment

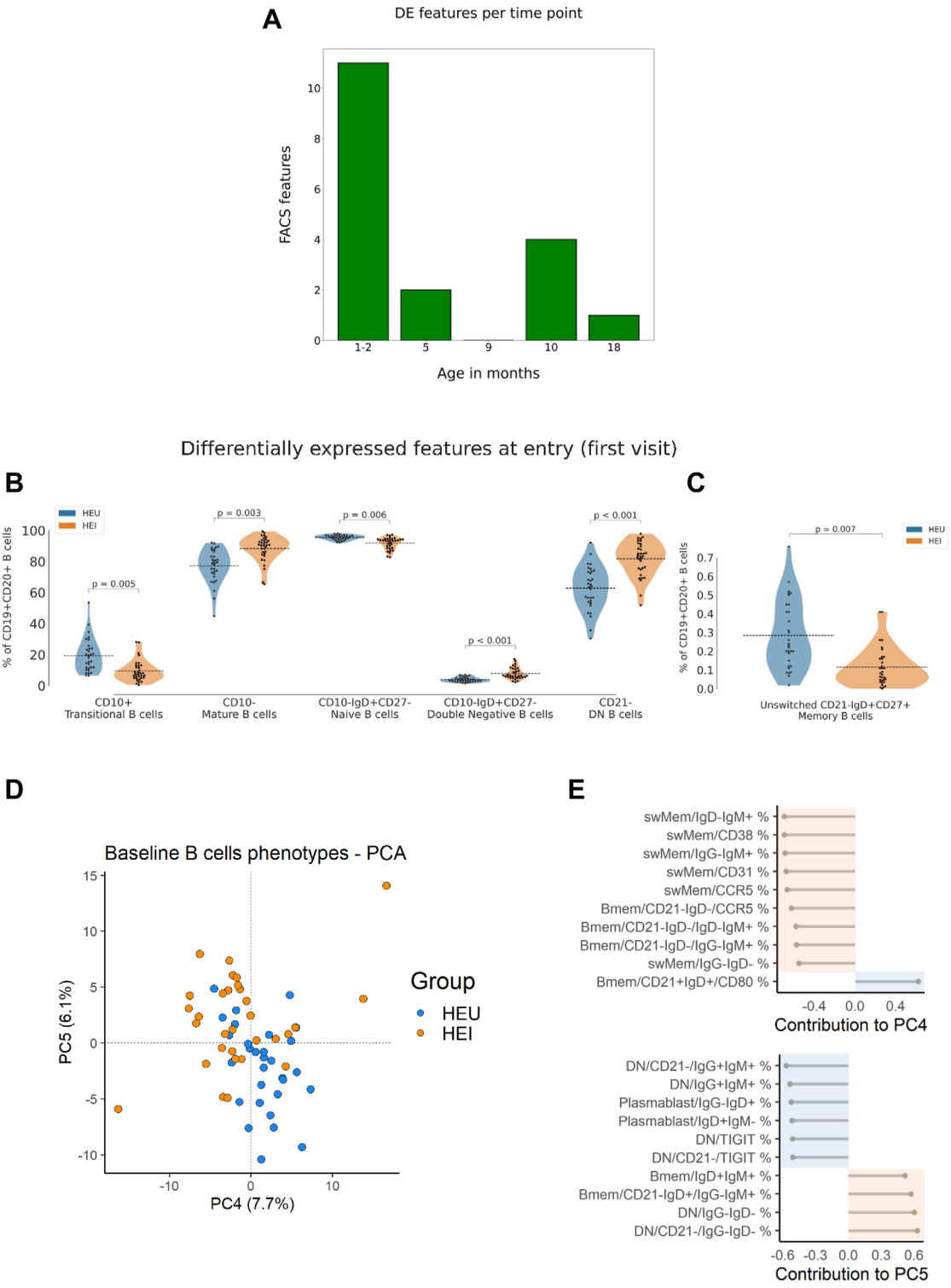

***Fig. 3:* B-cell phenotype of HEI and HEU in the first 2 years of life.** Bar plot in figure **A** shows the number of B-cell phenotype features (subsets) which resulted significantly different after Bonferroni correction (adj. p-value < 0.05) between HEU and HEI at each time point. Violin plots in panel **B** and **C** show the main distinctive features between HEU and HEI at entry, with mean values as black dotted lines. Principal component analysis (PCA) analyzing the B-cell phenotype at entry in HEU and HEI is shown in panel **D**. The first 10 top loading features contributing to PC4 and PC5 are shown in panel **E**.

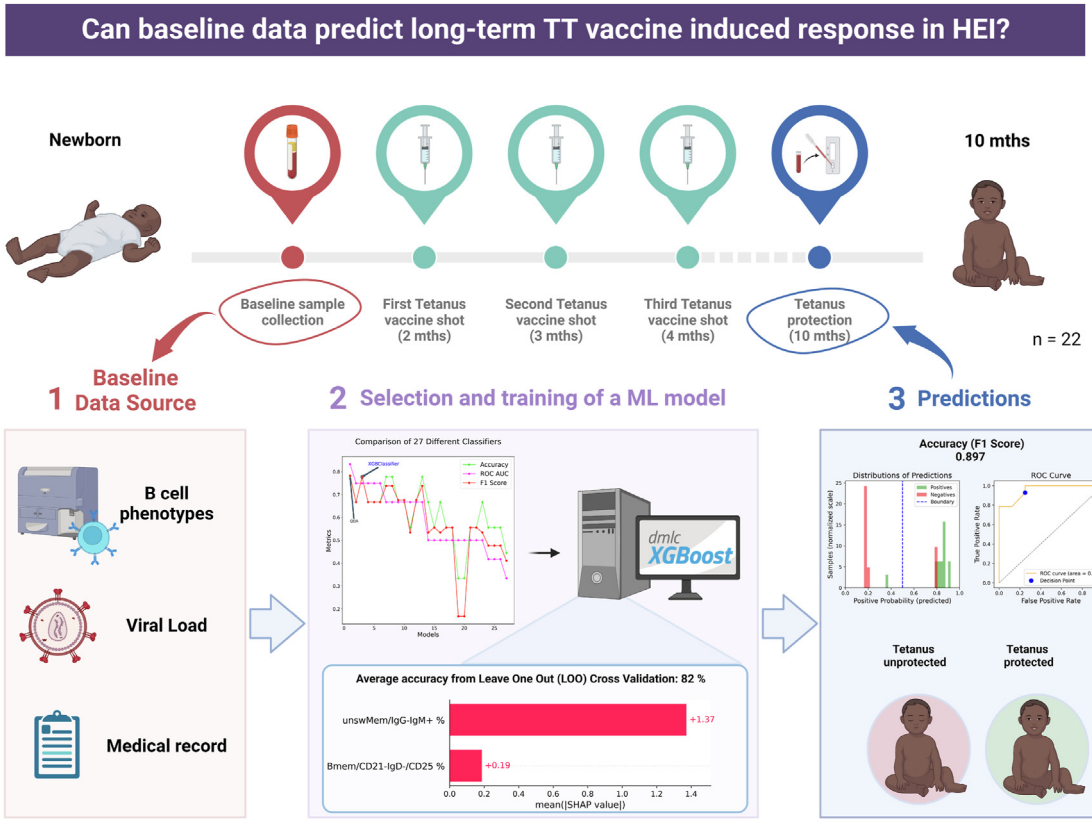

Fig. 4: **Prediction score of vaccine induced memory maintenance through a machine learning approach.** Panel 1 reports data sources used for model training. Panel 2 shows accuracy metrics (Accuracy in green, ROC AUC in magenta, and F1 score in red) of the classification algorithms tested on a 60/40 (train/test) split, together with the SHAP values expressing the feature importance scores for the optimized selected model. In panel 3 are reported the histogram of predictions and ROC curve of the model on the entire dataset (n = 22). Created with BioRender.com.

of the B-cells such as CD27+IgD–CD21–CD25+ and IgM+ unswitched memory B-cells. None of these cell subsets were found to be informative for either aging or in differentiating HEI from HEU.

Discussion

Children with perinatal HIV-infection present a lower ability to maintain vaccine induced immune protection.[19] However, the mechanisms of low immune response and the differential impact of maternal immune and virologic status, HIV progression and B-cell perturbation remain unknown especially in the very early phase of life. Here we characterized tetanus immune response and B-cell phenotype over the first 2 years of life, along with HIV progression in HEI as compared to HEU and HUU in order to investigate the efficacy of the current vaccination schedule for tetanus protection in children born in Mozambique and the B-cell characteristics underlying vaccination efficacy in this population. Despite an overall decrease in tetanus related morbidity and mortality, tetanus remains endemic in resource limited settings with the majority of tetanus-related deaths among newborn babies and mothers who have not been sufficiently immunized. Our data confirm that maternal derived protection at a mean age of 40 days is impaired in newborns with perinatal HIV with 50% of them being unprotected as compared to HEU (25% unprotected) and HUU (6.5% unprotected).[8,20]

Although previous studies have shown that a lower Ab transfer is more likely to be due to reduced maternal immunity rather than placental pathology or inflammation,[21] the role of HIV in this scenario has been only partially characterized.[22] This aspect has never been investigated in mother-child matched samples and longitudinally in children after childhood immunization. A study on women living with HIV and naïve to treatment showed a reduced IgG response compared to HIV uninfected individuals.[23] A distinct cross sectional study in children found a reduced TT seroprotection level in HEI compared with age-matched children without HIV[24] confirming the impact of the HIV status of both the mother and children on vaccine induced immunity. We further evaluated the impact of HIV status on the maternal Ab passage through a qualitative

analysis of distinct HIV Ab. Our data show that HEI and HEU in neonatal age differed in terms of HIV Ab. The ENV specific Ab for gp160 was positive in all HEI and in less than 40% of HEU, suggesting a distinct HIV Ab profile in HEI and possibly reflecting a diverse HIV status of the mothers at delivery. This result is also in line with a perturbed maternal passage of TT ab to HEI as compared to HEU. The opposite ratio was found for GAG specific Ab such as p17 and p55 which were mainly positive in HEU. In line with this, the HIV Ab repertoire at birth could represent an alternative diagnostic test in the screening of MTCT or HIV progression in these infants.[25]

Through the longitudinal characterization of the vaccine-induced Ab response we showed that HEI do not present a quantitative perturbation of the TT response immediately following immunization. However, in the long-term, our data showed a worse ability of HEI to maintain TT induced response compared to HEU, further supporting previous cross-sectional studies.[19]

The major impact of HIV on the ability of HEI to maintain TT immunity over time was investigated. Both HIV RNA and HIV Ab were significantly higher in TT unprotected HEI starting from 9 months of age. These data suggest that HIV exposure impacts the serologic ability to maintain Ab protective threshold over time, rather than playing a major role in the early response to vaccination. Overall, these data confirm the unreliability of the current vaccination schedule administered in Mozambique, which mirrors many African countries,[26] to ensure a protective Ab response upon tetanus especially in patients with low adherence and chronic viral replication.

The results presented here suggest that the adaptive cellular immunity compartment involving both long-term resting B and T cells may be the key factors to resolve the inability of these patients to keep long-term memory upon vaccination as compared to healthy controls.[27] In line with this, we wanted to define the timing of B-cell perturbation following HIV-infection characterizing the longitudinal evolution and maturation of the B-cell compartment in children with perinatal HIV infection. In contrast with the general idea that B-cell perturbation derives from a chronic and long-term exposure to HIV replication, we found that most distinguishing features of HEI compared to HEU were present at 40 days of life. The major differences found at baseline included a higher frequency of mature B-cells, and lower naïve and transitional B-cells in HEI compared to HEU, supporting a higher B-cell differentiation due to the acute infection. However, a distinctive feature between HEI and HEU was within the DN B-cells which were able to distinguish the groups at entry. This peculiar subset was described as a hallmark of B-cell exhaustion and aging, initially shown in elderly,[28] later in primary immunodeficiency and autoimmune diseases,[29–31] and more recently in people with HIV infection including children with vertical HIV-infection.[5,32] In this scenario, our data provide novel information on this B-cell paradoxical perturbation, characterized by a higher frequency in infants with HIV infection of a B-cell subset so far known to be increased in aging or inflamed conditions or in other infectious diseases such as cytomegalovirus or malaria, not tested in the present study. Matching these results at multiple time points we could show that the DN subset is the main driver of B-cell development in HEI with CD38+ and IgG+ DN B-cells inversely contributing to aging. This was not the case in HEU where mainly IgM+ IgG+ memory B-cells and CD21+ resting memory B-cells were contributing to B-cell development. Following the hypothesis that such perturbation may impact the ability of these children to maintain vaccine induced TT Abs, we explored whether baseline data could be fed into a machine learning approach to predict TT protection at 10 months. Our analysis was able to define a predictive score of long-term vaccine-induced protection according to B-cell subsets at entry. Of note, two distinct memory B-cell subsets were selected by the algorithm as informative. Instead, no subsets among the double negative B-cells or other immune senescent B-cell subsets were selected suggesting that "conventional" memory B-cells are involved in the vaccine induced memory maintenance in HEI. Albeit limited by the small sample size, the score was able to correctly predict 90% of participants (3 out of 22 were mispredicted). This approach may redirect immunization schedules in a subset of vulnerable patients in the future.

This study has some limitations. A broader serologic and clinical status of the mother is needed to better evaluate the significance of the findings at birth in these children. Despite providing novel data on TT Ab persistence in HEI, the same approach should be validated with other antigens included in the hexavalent vaccine using larger longitudinal cohort studies. In the context of machine learning, small sample size can be a potential limitation as it may not provide enough data to train a model effectively, leading to poor performance, high variance, and overfitting. A small sample size may also lead to a lack of diversity in the data, which can further impact the performance and generalizability of the model. In line with this, our results will need to be confirmed in larger cohorts and data sets.

Despite the aforementioned limitations, the present longitudinal study comprehensively determined the evolution of B-cells over the first 2 years of life in HEI as compared to HEU and describes the predominance of a B-cell perturbation in children living with HIV from the very early phases of life. It further confirms the impact of HIV on vaccine induced memory maintenance and suggests B-cell immune profiling may be used in the future as part of a predictive score able to personalize the vaccination schedule of HIV-infected children.

Contributors

All authors read and approved the final version of the manuscript. N.C., Su.P., M.S., M.G.L., P.P., and S.P. verified the data underlying the manuscript. Conceptualization, N.C., Su.P., L.D.A., P.P., and S.P.; methodology, V.D., S.R, S.D., and G.L.; software, M.S. and G.R.P.; formal analysis, M.S., N.C., and Su.P.; investigation, all authors including N.C., Su.P., M.S., V.D., L.d.A., S.R., S.D., G.L., G.R.P., R.P., N.S., P.V., P.R., M.G.L., P.P., and S.P.; resources, P.P. and S.P.; writing—original draft preparation, N.C. and Su.P.; writing—review and editing, all authors; supervision, P.P. and S.P.; funding acquisition, S.P., N.C., and P.P. All authors have read and agreed to the published version of the manuscript.

Data sharing statement

Original data and data supporting the findings of this study have been deposited to Mendeley Data: https://doi.org/10.17632/vhrbx46s97.1. All differentially expressed features between HEU and HEI are available on an online repository and deposited to Mendeley Data: https://doi.org/10.17632/b3d2p9fzg3.1. Scripts to reproduce the analyses presented in each figure of the paper are available at https://github.com/palma-lab/B_cells_immunity_manuscript.

Declaration of interests

All authors declare no conflict of interest.

Acknowledgements

This work was supported by a NIH grant to SP (5R01AI127347-05). Work performed at the Laboratory Sciences Core of the Miami was supported by CFAR P30AI073961 to University of Miami and by the following NIH Co-Funding and Participating Institutes and Centers: NIAID, NCI, NICHD, NHLBI, NIDA, NIMH, NIA, NIDDK, NIGMS, FIC, and OAR. Additional support was obtained by grants from Children's Hospital Bambino Gesú (Ricerca corrente 2019) to NC, and Associazione Volontari Bambino Gesù to PP. Funders had no role in study design, data collection, data analyses, interpretation, or writing of report. We thank Priya P. Ghanta for final review and edits to the manuscript.

Appendix A. Supplementary data

Supplementary data related to this article can be found at https://doi.org/10.1016/j.ebiom.2023.104666.

References

1 Thomas AS, Coote C, Moreau Y, et al. Antibody-dependent cellular cytotoxicity responses and susceptibility influence HIV-1 mother-to-child transmission. *JCI Insight*. 2022;7(9):e159435.
2 Cotugno N, Douagi I, Rossi P, Palma P. Suboptimal immune reconstitution in vertically HIV infected children: a view on how HIV replication and timing of HAART initiation can impact on T and B-cell compartment. *Clin Dev Immunol*. 2012;2012:1–11.
3 Cagigi A, Cotugno N, Giaquinto C, et al. Immune reconstitution and vaccination outcome in HIV-1 infected children: present knowledge and future directions. *Hum Vaccin Immunother*. 2012;8(12):1784–1794.
4 Frasca D, Pallikkuth S, Pahwa S. Metabolic phenotype of B cells from young and elderly HIV individuals. *Immun Ageing*. 2021;18(1):35.
5 Rinaldi S, Pallikkuth S, George VK, et al. Paradoxical aging in HIV: immune senescence of B Cells is most prominent in young age. *Aging*. 2017;9(4):1307–1325.
6 Kardava L, Moir S. B-cell abnormalities in HIV-1 infection: roles for IgG3 and T-bet. *Curr Opin HIV AIDS*. 2019;14(4):240–245.
7 Cotugno N, De Armas L, Pallikkuth S, et al. Perturbation of B Cell gene expression persists in HIV-infected children despite effective antiretroviral therapy and predicts H1N1 response. *Front Immunol*. 2017;8:1083.
8 Dolatshahi S, Butler AL, Siedner MJ, et al. Altered maternal antibody profiles in women with human immunodeficiency virus drive changes in transplacental antibody transfer. *Clin Infect Dis*. 2022;75(8):1359–1369.
9 Yen LM, Thwaites CL. Tetanus. *Lancet*. 2019;393(10181):1657–1668.
10 Lain MG, Vaz P, Sanna M, et al. Viral response among early treated HIV perinatally infected infants: description of a cohort in southern Mozambique. *Healthc Basel Switz*. 2022;10(11):2156.
11 Lain MG, Chicumbe S, Cantarutti A, et al. Caregivers' psychosocial assessment for identifying HIV-infected infants at risk of poor treatment adherence: an exploratory study in southern Mozambique. *AIDS Care*. 2023;35(1):53–62.
12 Rocca S, Zangari P, Cotugno N, et al. Human immunodeficiency virus (HIV)-antibody repertoire estimates reservoir size and time of antiretroviral therapy initiation in virally suppressed perinatally HIV-infected children. *J Pediatr Infect Dis Soc*. 2019;8(5):433–438.
13 Plotkin SA. Correlates of protection induced by vaccination. *Clin Vaccine Immunol*. 2010;17(7):1055–1065.
14 Chen T, Guestrin C. XGBoost: a scalable tree boosting system. In: *Proceedings of the 22nd ACM SIGKDD international conference on knowledge discovery and data mining*. San Francisco California USA: ACM; 2016:785–794. Available from: https://dl.acm.org/doi/10.1145/2939672.2939785. Accessed March 10, 2023.
15 Hastie T. *The elements of statistical learning: data mining, inference, and prediction*. 2nd ed. Springer; 2009.
16 Bergstra J. Making a science of model search: hyperparameter optimization in hundreds of dimensions for vision architectures. *PMLR*. 2013;28(1):115–123.
17 Guyon I, Weston J, Barnhill S, Vapnik V. Gene selection for cancer classification using support vector machines. *Mach Learn*. 2002;46(1/3):389–422.
18 Lundberg S, Lee SI. A unified approach to interpreting model predictions. *arXiv*; 2017. Available from: http://arxiv.org/abs/1705.07874. Accessed March 10, 2023.
19 Sutcliffe CG, Moss WJ. Do children infected with HIV receiving HAART need to be revaccinated? *Lancet Infect Dis*. 2010;10(9):630–642.
20 Baroncelli S, Galluzzo CM, Orlando S, et al. Immunoglobulin G passive transfer from mothers to infants: total IgG, IgG subclasses and specific antipneumococcal IgG in 6-week Malawian infants exposed or unexposed to HIV. *BMC Infect Dis*. 2022;22(1):342.
21 Wilcox CR, Holder B, Jones CE. Factors affecting the FcRn-mediated transplacental transfer of antibodies and implications for vaccination in pregnancy. *Front Immunol*. 2017;8:1294.
22 Bebell LM, Siedner MJ, Ngonzi J, et al. Brief report: chronic placental inflammation among women living with HIV in Uganda. *J Acquir Immune Defic Syndr*. 2020;85(3):320–324.
23 Dieye TN, Sow PS, Simonart T, et al. Immunologic and virologic response after tetanus toxoid booster among HIV-1- and HIV-2-infected Senegalese individuals. *Vaccine*. 2001;20(5–6):905–913.
24 Simani OE, Izu A, Violari A, et al. Effect of HIV-1 exposure and antiretroviral treatment strategies in HIV-infected children on immunogenicity of vaccines during infancy. *AIDS*. 2014;28(4):531–541.
25 Palma P, McManus M, Cotugno N, Rocca S, Rossi P, Luzuriaga K. The HIV-1 antibody response: a footprint of the viral reservoir in children vertically infected with HIV. *Lancet HIV*. 2020;7(5):e359–e365.
26 Why CDC is working to prevent global tetanus [internet]. Available from: https://www.cdc.gov/globalhealth/immunization/diseases/tetanus/why/index.html. Accessed October 25, 2022.
27 Amanna IJ, Carlson NE, Slifka MK. Duration of humoral immunity to common viral and vaccine antigens. *N Engl J Med*. 2007;357(19):1903–1915.
28 Colonna-Romano G, Bulati M, Aquino A, et al. A double-negative (IgD–CD27–) B cell population is increased in the peripheral blood of elderly people. *Mech Ageing Dev*. 2009;130(10):681–690.
29 Wang W, Min Q, Lai N, et al. Cellular mechanisms underlying B cell abnormalities in patients with gain-of-function mutations in the PIK3CD gene. *Front Immunol*. 2022;13:890073.
30 Cotugno N, Finocchi A, Cagigi A, et al. Defective B-cell proliferation and maintenance of long-term memory in patients with chronic granulomatous disease. *J Allergy Clin Immunol*. 2015;135(3):753–761.e2.
31 Hardt U, Carlberg K, af Klint E, et al. Integrated single cell and spatial transcriptomics reveal autoreactive differentiated B cells in joints of early rheumatoid arthritis. *Sci Rep*. 2022;12(1):11876.
32 Ruggiero A, Pascucci GR, Cotugno N, et al. Determinants of B-cell compartment hyperactivation in European adolescents living with perinatally acquired HIV-1 after over 10 years of suppressive therapy. *Front Immunol*. 2022;13:860418.